Correspondence

Combination of e-Beam Lithography and of High Velocity AlN/Diamond-Layered Structure for SAW Filters in X Band

Philippe Kirsch, Mohamed B. Assouar, Omar Elmazria, M. El Hakiki, Vincent Mortet, and Patrick Alnot

***Abstract*—In this work, we report on the fabrication results of surface acoustic wave (SAW) devices operating at frequencies up to 8 GHz. In previous work, we have shown that high acoustic velocities (9 to 12 km/s) are obtained from the layered AlN/diamond structure. The interdigital transducers (IDTs) made of aluminium with resolutions up to 250 nm were successfully patterned on AlN/diamond-layered structures with an adapted technological process. The uniformity and periodicity of IDTs were confirmed by field emission scanning electron microscopy and atomic force microscopy analyses. A highly oriented (002) piezoelectric aluminum nitride thin film was deposited on the nucleation side of the CVD diamond by magnetron sputtering technique. The X-ray diffraction effectuated on the AlN/diamond-layered structure exhibits high intensity peaks related to the (002) AlN and (111) diamond orientations. According to the calculated dispersion curves of velocity and the electromechanical coupling coefficient (K^2), the AlN layer thickness was chosen in order to combine high velocity and high K^2. Experimental data extracted from the fabricated SAW devices match with theoretical values quite well.**

I. Introduction

SURFACE acoustic wave (SAW) devices, initially developed for electrical filter applications [1]–[3], have become more and more important during the last decades. Considering all the advantages of such devices, efforts have been made during the last decade to extend their application range to gas [4], [5] and liquid sensing applications [6], [7].

There has been a drastic improvement in their performances as well as in their domains of application. The operating frequency of SAW devices is directly proportional to the acoustic wave velocity of the considered structure and considered mode, and inversely proportional to the spatial periodicity of the interdigital transducers (IDTs). SAW devices operating in the X band for communication systems require combinations of submicron or nanometric IDTs [8] and high acoustic velocity substrates. The highest frequency SAW devices are expected from diamond substrates with an aluminium nitride piezoelectric layer, because diamond presents the highest acoustic wave velocity among all materials [9], and aluminium nitride has a very high acoustic wave velocity, in comparison to other piezoelectric materials. AlN film also exhibits a good piezoelectric coupling coefficient along its c-axis [10]. Theoretical analysis of the AlN, ZnO/diamond substrates [11] show the high velocities. In previous work, we have demonstrated experimentally that the diamond/AlN structure exhibits phase velocities up to 12 km/s [11], [12]. E-beam lithography (EBL) is one of the most versatile techniques for the fabrication of submicron and nanometric structures [8], [13]–[15]. Hence, the EBL technique is an attractive solution for the development of prototype devices. Resolutions down to 20 nm are obtained on silicon with low density patterns [16], [17]. However, EBL used for piezoelectric materials such as aluminum nitride must deal with difficulties arising from its high electrical resistivity. Moreover, IDT structures exhibit nonsymmetrical geometry with a large length (0.1 to 1 mm), submicron lines, and a very dense pattern. One of the common methods to overcome these drawbacks consists in evaporating a thin metal layer over the e-beam sensitive resist layer, and connecting this metal to the electrical ground of the e-beam system [16], [17]. Another technique consists in the deposition of an antistatic agent on the resist to evacuate the charges [15]. In this work, we present a method to overcome the charge accumulation problem using a thin charge evacuation layer deposited on top of the resist [8]. A lift-off process is used to pattern the electrodes [13], and it should be carefully combined with EBL for the realization of SAW devices. This paper first describes the fabrication process of SAW devices using EBL and lift-off technique. This process allows the achievement of well-defined IDT finger patterns with a line width down to 250 nm. Second, in this work, we present, the frequency responses of SAW devices obtained using this fabrication process, which exhibits a very high operating frequency, around 8 GHz. This work points out the technological process for EBL on high-resistivity piezoelectric materials and the realization of high-frequency functional SAW devices based on AlN/diamond layered structures.

Manuscript received February 13, 2007; accepted March 27, 2007.

P. Kirsch, M. B. Assouar, O. Elmazria, M. El Hakiki, and P. Alnot are with the Laboratoire de Physique des Milieux Ionisés et Applications, LPMIA, Nancy University - CNRS, Nancy, France (e-mail: badreddine.assouar@lpmi.uhp-nancy.fr).

V. Mortet is with the Institute for Materials Research-Limburgs Universitair Centrum, Wetenschapspark 1-B-3590 Diepenbeek, Belgium.

Digital Object Identifier 10.1109/TUFFC.2007.411

II. Experimental Setup

The present submicron fabrication process was applied to the realization of high-frequency SAW devices based on a 1 μm piezoelectric aluminum nitride layer, deposited on the nucleation side of the free standing diamond substrates. The size of the diamond substrates used is 10 mm, 10 mm, and 0.1 mm.

A. Diamond Substrate

Polycrystalline diamond films were grown on silicon wafers by plasma-enhanced chemical vapor deposition (PECVD), using an ASTeX reactor operating at a microwave power of 6 kW and a pressure of 160 mbar, with a volume mixture of 3% of CH_4 in H_2 [12]. After deposition, the polycrystalline diamond layer was removed from the silicon substrate by a wet chemical etch in HNA solution ($HF:HNO_3:CH_3COOH$), leading to a freestanding diamond layer with a flat surface on the nucleation side. The nucleation side of the freestanding diamond surface is smooth with an average root-mean-square roughness R_{rms} of 1 nm, determined by nucleation density and by the surface quality of sacrificial wafer.

B. Aluminum Nitride Deposition

AlN thin films were prepared by reactive RF magnetron sputtering on CVD substrates. The experimental growth conditions of our process were published elsewhere [18], [19]. The growth rate is 0.5 μm/hour. The film thickness was measured by field emission scanning electron microscopy (FESEM) using a cross section of the structure.

C. Realization Process

The electrosensitive resist used in our process is a double layer consisting of two different electrosensitive resists: MMA and 950 K PMMA from Micro Chem. The first resist spun onto the substrate is the MMA copolymer. Right after the spin coating of the substrate, it is baked for 1 hour at 160°C. Then, the 950 K PMMA resist is spun onto the substrate, and the substrates is baked for 1 more hour at 160°C. Both resists were spun with the same experimental conditions. The double layer of resist is used to facilitate the lift-off process step. In fact, the MMA resist is more sensitive than the PMMA resist. Hence, for a given exposure dose, the aperture in the MMA layer will be wider than in the PMMA layer after development. This induces an under-cut profile in the resist double-layer itself. The resulting thickness of the resist layers is 225 nm for the MMA resist and 75 nm for the PMMA resist. As the substrate material combination used is electrically rather insulating, and to overcome the charge accumulation on the surface of the substrate [20], a 10 nm layer of gold was deposited by thermal evaporation on top of the resist.

After this step, the EBL is carried out on a field emission scanning electron microscope (JEOL JSM-6500F) modified to accommodate a DEBEN PCD Beam Blanker. The whole system is controlled by RAITH Advanced SEM/FIB Nanolithography System hardware and RAITH Quantum software. The lithography was done at an acceleration voltage of 30 kV and a current of 55 pA. The exposure dose for each structure strongly depends on its size and on its geometrical aspect. The used doses range from 200 $\mu C/cm^2$ up to 500 $\mu C/cm^2$. After the exposure of the IDT structures, the gold charge evacuation layer is selectively etched away using a KI/I_2 solution. The resists' development is done by rinsing the exposed substrate into a methyl-isobuthyl-ketone: Isopropanol (1:3) solution for 60 seconds. The development process is stopped by rinsing the substrate in pure Isopropanol for another 60 seconds. The substrate is then quickly dried using a dry nitrogen flow.

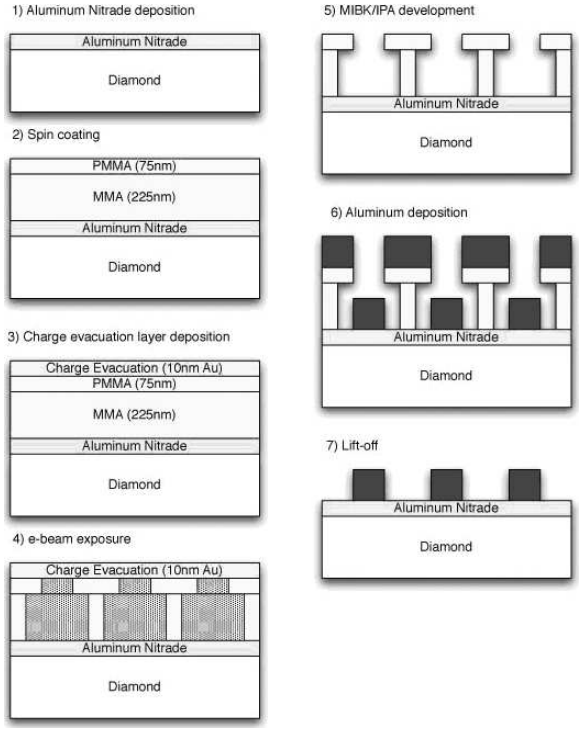

Fig. 1. SAW realization process.

The resist double layer is now structured, and a 100 nm aluminum layer is deposited onto the top surface by thermal evaporation. The deposition occurs at about 10^{-6} mbar, the deposition rate is 1.2 Å/s. After the aluminum deposition, a lift-off is performed to set the IDT structures free. Fig. 1 shows the different process steps of the e-beam lithography based lift-off technique.

III. Results and Discussion

Several SAW devices with submicron features were made using the technological process previously described. SAW devices with various spatial periodicities from 1 μm to 3.2 μm have been made. The corresponding finger widths vary from 250 nm to 800 nm. For all these devices, the aperture is fixed to 90 μm, and the gap between the IDT emitter and receiver is fixed to 20 μm, except for the device with the lowest spatial resolution of 1.2 μm, in which the gap is fixed to 10 μm, and the aperture is fixed to 80 μm. Each IDT consists of 50 pairs of fingers. The devices made with 250 and 300 nm lateral resolution were performed with two geometric features, 50 and 75 finger pairs. We presented in this paper only the results concerning the design with 75 finger pair. The same results were obtained for 50 pairs of finger.

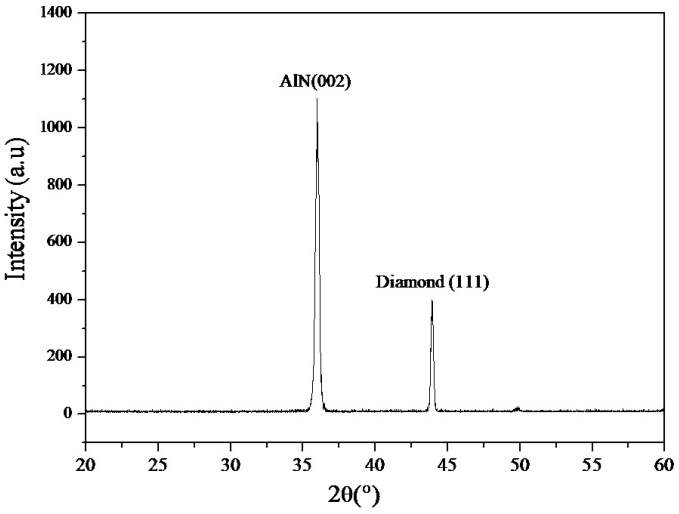

Fig. 2. XRD spectrum in θ–2θ scan mode of AlN film deposited on the nucleation side of the PECVD diamond substrate.

In the case of the IDTs structure, the proximity effect constitutes the main difficulty in the EBL technique [21], [22]. After a series of process optimizations, the proximity effect could be overcome by using a nonhomogeneous exposure technique. This technique consists in modulating the real dose of the exposure, depending on the geometry, size, and density of the structure [23].

Structural characterizations of AlN/diamond-layered structures were carried out by X-ray diffraction (XRD). Fig. 2 shows the XRD in θ–2θ scan mode for the AlN film deposited on the nucleation side of the CVD diamond substrate. The deposited AlN film is highly oriented on (002), which means that the c-axis of the AlN is perpendicular to the substrate surface. The diamond substrate itself also shows a high degree of orientation on (111). The control of the quality and of the IDTs resolutions were carried out by FESEM and atomic force microscopy (AFM) analysis. Fig. 3(a) shows a FESEM image of a realized SAW device with an IDT of 300 nm finger widths. The regularity of the IDTs is rather good, although there are local imperfections, as well as a nonnegligible surface roughness of the IDT fingers that can be observed. The FESEM image gives quite a good representation of the top aspect of the fabricated SAW, but there is no information available about the thickness, regularity, or definition of the IDTs. Therefore, AFM was used to characterize the fabricated structures.

During the evolution and improvement of the fabrication process, smooth and regular IDTs have been obtained. This was achieved by decreasing the aluminum deposition rate to 1.2 Å/s and using an appropriate crucible allowing a constant deposition rate during the deposition process. Adding 30 s to the ultrasonic bath at the end of the lift-off process improved it and allowed the realization of the first operational devices [Fig. 3(a)].

Fig. 3(b) shows the AFM image, which presents the results of all the process improvements applied. One can observe a regular spatial periodicity of the IDT fingers, and a very regular IDT thickness. Despite the improvements achieved, the proximity effects are still problematic when finger widths smaller resolutions on very high resistivity substrates.

After the structural analysis, we have proceeded to the frequency characterization of the SAW devices obtained, using an Agilent 8752A network analyzer and an RF microprober (Suss Microtech). The first device based on an AlN/diamond structure has been realized with a wavelength of 2.4 μm corresponding to lateral IDT resolution of 600 nm. The finger width: inter-finger distance ratio is 1:2. The thickness of AlN film used for the SAW structure is 1 μm. Then, the normalized thickness kh (where k is the wavenumber and h is the thickness of the AlN film) for this device is 2.61, taking into account the wavelength of 2.4 μm. In Fig. 4, one can observe the frequency response of this SAW device, which exhibits three peaks related to different acoustic propagation modes in the AlN/diamond-layered structure. The first peak located at 3.89 GHz (Mode 1) corresponds to a propagation mode with a phase velocity of 9336 m/s, which is close to the theoretical one (9749 m/s) [24]. The second peak located at 4.67 GHz (Mode 2) corresponds to a phase velocity of 11200 m/s, which is hardly different to the theoretical value of 11890 m/s. This very slight difference between experimental and theoretical values of phase velocity is due to the fact that, in our calculations, we do not have taken into account the mass loading effect of aluminium IDTs, which induces the decreasing of phase velocity. Otherwise, a good filtering performance of this SAW device, when Mode 1 is considered, was obtained: relatively low insertion loss (less than 31 dB) at the center frequency (f = 3.89 GHz), and more than 20 dB of stop band rejection. The low intensity of the Mode 2 peak and the absence of the Mode 0 peak, which are generally generated in the AlN/diamond-layered structure, are explained by the low electromechanical coupling coefficient values of these modes at this normalized thickness of 2.61. In fact, the K^2 values are near zero for Mode 0 and 0.022% for Mode 2 [24]. We can note that no particular design of IDTs was performed to improve the rejection or to limit the insertion loss.

The second SAW device we performed was made with a 300 nm lateral resolution IDTs on a layered structure. One can observe in Fig. 5 the frequency response of this second SAW device with a wavelength of 1.2 μm. We observe two peaks, of which the first one (Mode 1) is located at 6.7 GHz, and corresponds to a propagation mode with a phase velocity of 8040 m/s. Knowing that the normalized thickness kh of this second structure is 5.23 (1 μm AlN thickness), the theoretical value of phase velocity of this mode is 8473 m/s [24]. The second peak observed in Fig. 5 located at 7.7 GHz, corresponds to the Mode 2 with a phase velocity of 9300 m/s, which is very slightly different to the theoretical value of 10,000 m/s. These differences between experimental and theoretical phase velocity values are due, as we said before, to the loading mass effect inducing by aluminium thickness. Concerning Mode 0, al-

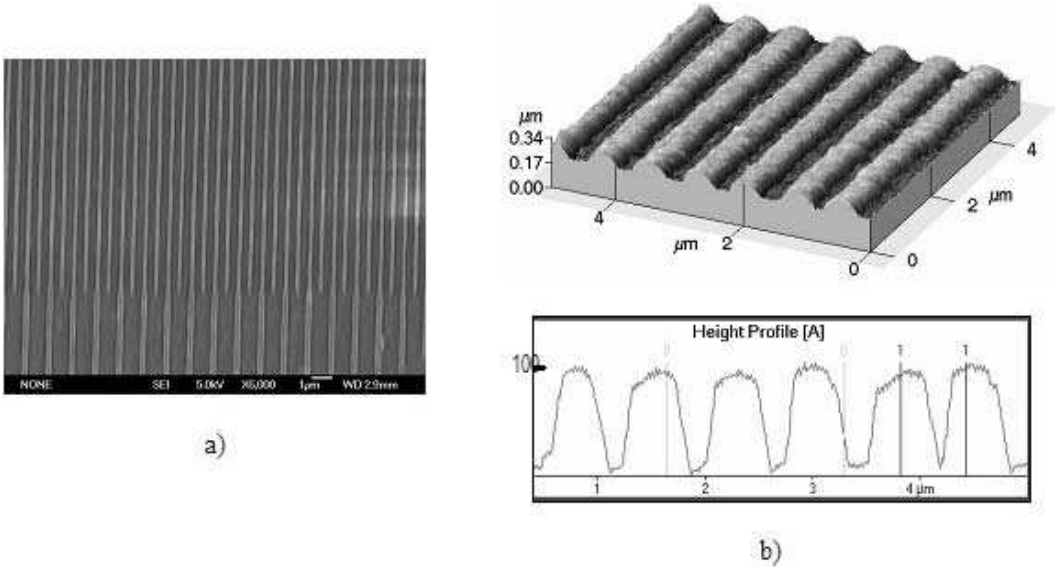

Fig. 3. (a) FESEM image of an IDT structure of 300 nm. (b) 3-D AFM image showing the good profile regularity of the realized IDT structure, and AFM profile confirming the aluminum thickness.

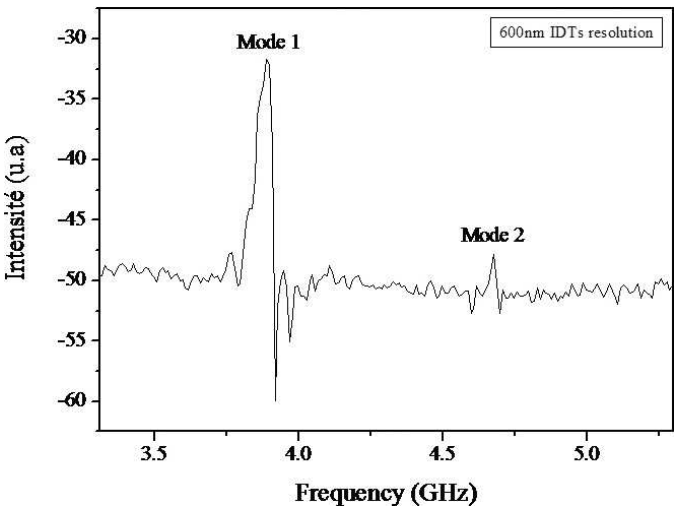

Fig. 4. Frequency response of a SAW device of wavelength 2.4 μm.

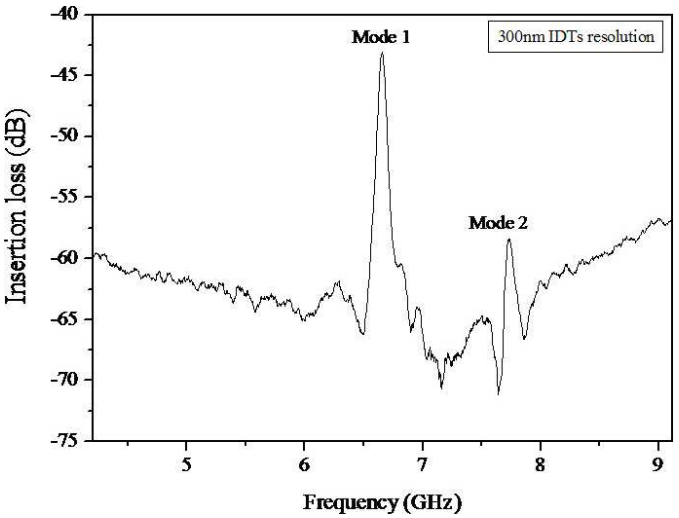

Fig. 5. Frequency response of a SAW device of wavelength 1.2 μm.

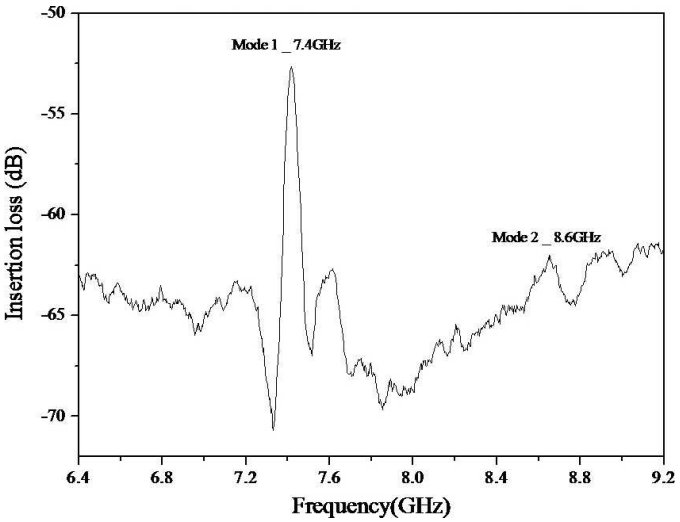

Fig. 6. Frequency response of a SAW device of wavelength 1 μm.

though expected by numerical simulations, the peak of this mode could not be found during measurements.

To achieve 8 GHz operating frequency, we present in Fig. 6, a last SAW device realized with a 250 nm lateral resolution, corresponding to 1 μm wavelength. The observed peaks correspond to the Mode 1 and 2 with velocities of 7410 m/s and 8640 m/s, respectively. The theoretical ones are 7909 m/s and 9530 m/s, respectively, for Modes 1 and 2. The difference between these experimental and theoretical values achieves 9%. This difference is between 4% and 7% for the two first devices. We can deduce that the difference between the experimental and theoretical values of phase velocity increase with decreasing the wavelength. This result confirms that this difference is due mainly to the loading mass effect of aluminium thickness.

In this work, the experimental K^2 coefficient was determined using measured data of the S_{11} parameter (re-

flection) and using the following equation derived from Smith's equivalent model [24], [25]:

$$K^2 = \frac{G(f_0)}{8.f_0.C.N^2} = \frac{\pi}{4N}\frac{G(f_0)}{B(f_0)},$$

where $G(f_0)$ and $B(f_0)$ are, respectively, the radiation conductance and susceptance measured by network analyzer Smith chart at center frequency f_0, C the capacitance between an IDT finger pair of interdigital transducer, and N the number of finger pairs of IDT.

For the second device with a normalized kh value of 5.23, we found a value of 1.37%. This value is higher than the theoretical one, which is equal to 1.02% with regard to the dispersion curve of the electromechanical coupling coefficient published elsewhere [11], [26]. The theoretical calculations underestimate the K^2 value as mentioned in the studies of Adler and Solie [26]. They showed that the electromechanical coupling coefficient calculated at a constant frequency is about four times larger than that calculated at a constant wavelength. This method was used in our study. Wu and Chen [27] showed, by an exact analysis using effective permittivity to calculate K^2 in a ZnO/diamond structure, the obtaining of a theoretical value higher than the theoretical one obtained using the Adler and Solie approach [26], and the obtained value agreed well with the measurements reported by Nakahata *et al.* for a ZnO/diamond layered structure [28]. We also can explain the difference between theoretical and experimental values of K^2 by the fact, that in the theoretical calculations, we do not take into account the mass loading effects of aluminum thickness. In experimental approaches, this effect is observed and the increasing of K^2 is also due to the aluminum grating that operates as resonator.

The temperature coefficient of frequency (TCF) measurement of SAW devices was done in order to evaluate the temperature stability of such a very high frequency device. Fig. 7 shows the dependence of frequency to the temperature that gives a TCF value of -9 ppm/°C of the SAW device achieved with a 2.4 μm wavelength. This value remains small, and can be reduced with an SiO_2 thin layer compensation, or by increasing the AlN film thickness, because AlN and diamond films have opposite TCF signs [1]. This second solution should be carried out taking into account that we will induce a slight phase velocity decrease in the layered structure. The best compromise between the higher phase velocity and the lowest TCF has to be found.

IV. Conclusions

A gigahertz SAW device operating at frequencies up to 8 GHz was performed on an AlN/diamond multilayer structure using EBL combined with a lift-off process. The technological process was pointed out for high electrical resistivity materials in order to overcome electrons accumulation on the substrate surface. The proximity effects were avoided by adjusting the dose injected in the resist and by the nonuniform dose exposure of the pattern. The obtained results show the good quality of the operating SAW device achieved using the developed technological process. The lateral resolution of 250 nm was reached. The obtained frequency responses showed very interesting frequency characteristics, and pointed out the different propagation modes in concordance with the theoretical values of acoustic velocities and electromechanical coupling coefficients. The combination of high acoustic velocity materials such as diamond and the EBL technique allows realization of SAW devices operating at frequencies up to 8 GHz.

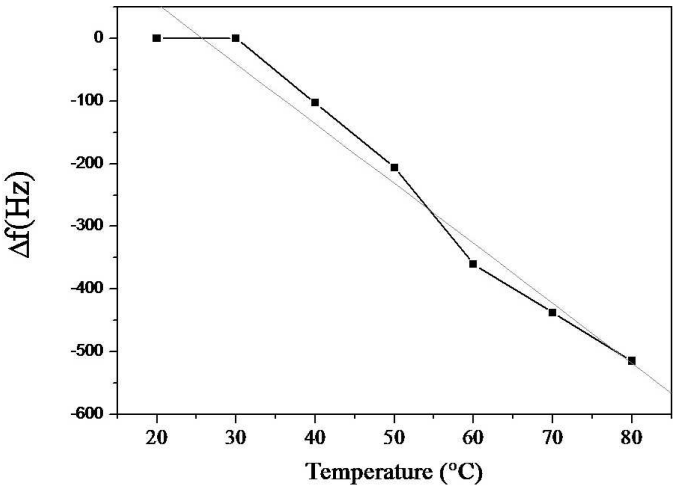

Fig. 7. Temperature coefficient frequency of SAW device with 2.4 μm wavelength.

References

[1] O. Elmazria, V. Mortet, M. El Hakiki, M. Nesladek, and P. Alnot, "Velocity SAW using aluminum nitride film on unpolished nucleation side of free-standing CVD diamond," *IEEE Trans. Ultrason., Ferroelect., Freq. Contr.*, vol. 50, no. 6, pp. 710–715, 2003.

[2] M. B. Assouar, F. Bénédic, O. Elmazria, M. Belmahi, R. Jiménez-Riobóo, and P. Alnot, "Modelling of SAW filter based on ZnO/diamond/Si layered structure including velocity dispersion," *Diam. Relat. Mater.*, vol. 10, pp. 681–685, 2001.

[3] M. B. Assouar, O. Elmazria, M. El Hakiki, P. Alnot, and C. Tiusan, "Low temperature AlN thin films growth for layered structure SAW and BAW devices," in *Proc. IEEE Int. Symp. Appl. Ferroelect. ISAF04*, 2004, pp. 43–46.

[4] M. El Hakiki, O. Elmazria, M. B. Assouar, V. Mortet, L. Le Brizoual, M. Vanecek, and P. Alnot, "ZnO/AlN/diamond layered structure for SAW devices combining high velocity and high electromechanical coupling coefficient," *Diam. Relat. Mater.*, vol. 14, pp. 1175–1178, 2005.

[5] J. Wagner and K. von Schickfus, "Inductively coupled, polymer coated surface acoustic wave sensor for organic vapors," *Sens. Actuators B*, vol. 76, pp. 58–63, 2001.

[6] J. Kondoh, T. Muramatsu, T. Nakanishi, Y. Matsui, and S. Shiokawa, "Development of practical surface acoustic wave liquid sensing system and its application for measurement of Japanese tea," *Sens. Actuators B*, vol. 92, pp. 191–198, 2003.

[7] F. Martin, M. I. Newton, G. McHale, K. A. Melzak, and E. Gizeli, "Pulse mode shear horizontal-surface acoustic wave (SH-SAW) system for liquid based sensing applications," *Biosens. Bioelectron.*, vol. 19, pp. 627–632, 2004.

[8] K. Yamanouchi, Y. Chou, and T. Meguro, "SHF-range surface acoustic wave inter-digital transducers using electron beam exposure," in *Proc. IEEE Ultrason. Symp.*, 1988, pp. 115–118.

[9] A. J. Slobodnik and E. D. Conway, "Microwave Acoustics Handbook," vol. 1, U.S. Air Force Cambridge Research Laboratories, Report No. AFCRL-PSRP-414, Accession no. AD 868360, 1970.
[10] T. Shiosaki, K. Harada, and A. Kawabata, "Low-temperature growth of the piezoelectric AlN film and its optical and acoustical properties," in *Proc. IEEE Ultrason. Symp.*, 1981, pp. 506–509.
[11] K. Yamanouchi, N. Sakurai, and T. Satoh, "SAW propagation characteristics and fabrication technology of piezoelectric thin film/diamond structure," in *Proc. IEEE Ultrason. Symp.*, 1989, pp. 351–354.
[12] M. El Hakiki, O. Elmazria, M. B. Assouar, V. Mortet, L. Le Brizoual, M. Vanecek, and P. Alnot, "ZnO/AlN/diamond layered structure for SAW devices combining high velocity and high electromechanical coupling coefficient," *Diam. Relat. Mater.*, vol. 14, pp. 1175–1178, 2005.
[13] H. I. Smith, "Surface acoustic wave devices fabrication," in *Surface Acoustic Wave Filters*. H. Matthews, Ed. New York: Wiley, 1977, pp. 165–217.
[14] K. Yamanouchi, "On acoustic wave devices for future mobile communication systems," in *Proc. Second Int. Symp. Acoust. Wave Devices Future Mobile Commun. Syst.*, 2004, pp. 1–8.
[15] H. Hatakeyama, T. Omori, K.-Y. Hashimoto, and M. Yamaguchi, "Fabrication of SAW devices using SEM-based electron beam lithography and lift-off technique for lab use," in *Proc. IEEE Int. Ultrason., Ferroelect., Freq. Contr. Joint 50th Anniversary Conf.*, 2004, pp. 1896–1900.
[16] T. Palacios, F. Calle, E. Monroy, and E. Muñoz, "Submicron technology for III-nitride semiconductors," *J. Vac. Sci. Technol. B*, vol. 20, no. 5, pp. 2071–2074, 2002.
[17] P. Rai-Choudhury, Ed. *Handbook of Microlithography, Micromachining and Microfabrication*. London: SPIE, 1997.
[18] M. B. Assouar, M. El Hakiki, O. Elmazria, P. Alnot, and C. Tiusan, "Synthesis and microstructural characterisation of reactive RF magnetron sputtering AlN films for surface acoustic wave filters," *Diam. Relat. Mater.*, vol. 13, pp. 1111–1115, 2004.
[19] T. Easwarakhanthan, M. B. Assouar, P. Pigeat, and P. Alnot, "Optical models for radio-frequency-magnetron reactively sputtered AlN films," *J. Appl. Phys.*, vol. 98, pp. 073531-1–073531-7, 2005.
[20] T. Palacios, F. Calle, E. Monroy, J. Grajal, M. Eickhoff, O. Ambacher, and C. Prieto, "Nanotechnology for SAW devices on AlN epilayers," *Mater. Sci. Eng. B*, vol. 93, pp. 154–158, 2002.
[21] F. Lehmann, G. Richter, T. Borzenko, V. Hock, G. Schmidt, and L. W. Molenkamp, "Fabrication of sub-10-nm Au-Pd structures using 30 keV electron beam lithography and lift-off," *Microelectron. Eng.*, vol. 65, pp. 327–333, 2003.
[22] Y. M. Gueorguiev, K. G. Vutova, and G. M. Mladenov, "A Monte Carlo study of proximity effects in electron-beam patterning of high-T_c superconducting thin films," *Physica C*, vol. 249, pp. 187–195, 1995.
[23] P. Kirsch, M. B. Assouar, O. Elmazria, C. Tiusan, and P. Alnot, "5GHz SAW devices based on AlN/diamond layered structure," in *Proc. IEEE Int. Symp. Appl. Ferroelect.*, 2006, pp. 2293–2296.
[24] J. H. Hines and D. C. Malocha, "A simple equivalent circuit parameter extraction technique," in *Proc. IEEE Ultrason. Symp.*, 1993, pp. 173–177.
[25] F. Jungnickel and H.-J. Fröhlich, "Determination of transducer equivalent circuit and the coupling coefficient in SAW structures," *Acoust. Ultrason. Proc. 12th Eur. Conf. Eurosensors XII*, 1998, pp. 89–92.
[26] E. L. Adler and L. Solie, "ZnO on diamond SAWs and pseudo-SAWs," in *Proc. IEEE Ultrason. Symp.*, 1995, pp. 341–344.
[27] T. Wu and Y.-Y. Chen, "Exact analysis of dispersive SAW devices on ZnO/diamond/Si-layered structures," *IEEE Trans. Ultrason., Ferroelect., Freq. Contr.*, vol. 49, no. 1, pp. 142–149, 2002.
[28] H. Nakahata, K. Higaki, S. Fujii, A. Hachigo, H. Kitabayashi, K. Tanabe, Y. Seki, and S. Shikata, "SAW devices on diamond," in *Proc. IEEE Ultrason. Symp.*, 1995, pp. 361–370.